Insect Systematics and Diversity, (2022) 6(1): 11; 1–17
https://doi.org/10.1093/isd/ixab029
Research

ENTOMOLOGICAL SOCIETY OF AMERICA
SHARING INSECT SCIENCE GLOBALLY

OXFORD

Molecular Phylogenetics, Phylogenomics, and Phylogeography

The Last Piece of the Puzzle? Phylogenetic Position and Natural History of the Monotypic Fungus-Farming Ant Genus *Paramycetophylax* (Formicidae: Attini)

Priscila Elena Hanisch,[1,3,†] Jeffrey Sosa-Calvo,[2,3,†] and Ted R. Schultz[2]

[1]Department of Ornithology, Museo Argentino de Ciencias Naturales 'Bernardino Rivadavia' MACN-CONICET, Buenos Aires, Argentina, [2]Department of Entomology, National Museum of Natural History, Smithsonian Institution, Washington DC, USA, and [3]Corresponding author, e-mails: sossajef@si.edu; hanisch.priscila@gmail.com

[†]The two first authors contributed equally to this paper.

Subject Editor: Gabriela P Camacho

Received 2 August 2021; Editorial decision 3 November 2021

Abstract

The evolutionary history of fungus-farming ants has been the subject of multiple morphological, molecular phylogenetic, and phylogenomic studies. Due to its rarity, however, the phylogenetic position, natural history, and fungal associations of the monotypic genus *Paramycetophylax* Kusnezov have remained enigmatic. Here we report the first excavations of colonies of *Paramycetophylax bruchi* (Santschi) and describe its nest architecture and natural history. Utilizing specimens from these collections, we generated ultraconserved-element (UCE) data to determine the evolutionary position of *Paramycetophylax* within the fungus-farming ants and ribosomal 'fungal barcoding' *ITS* sequence data to identify the fungal cultivar. A maximum-likelihood phylogenomic analysis indicates that the genus *Paramycetophylax* is the sister group of the yeast-cultivating *Cyphomyrmex rimosus* group, an unexpected result that renders the genus *Cyphomyrmex* Mayr paraphyletic. A Bayesian divergence-dating analysis indicates that *Paramycetophylax* diverged from its sister group around 36 mya (30–42 mya, HPD) in the late Eocene-early Oligocene, a period of global cooling, expansion of grasslands, and large-scale extinction of tropical organisms. Bayesian analysis of the fungal cultivar *ITS* gene fragment indicates that *P. bruchi* practices lower agriculture and that the cultivar grown by *P. bruchi* belongs to the Clade 1 group of lower-attine fungi, a clade that, interestingly, also includes the *C. rimosus*-group yeast cultivars. Based on these results, we conclude that a better understanding of *P. bruchi* and its fungal cultivar, including whole-genome data, is critical for reconstructing the origin of yeast agriculture, a major transition in the evolution of fungus-farming ants.

Key words: ant agriculture, fungus-growing ant, nest architecture, phylogenomics, ultraconserved element

The fungus-farming ants (family Formicidae: tribe Attini in part; here regarded as the 'Attina', an informal subtribal grouping, and referred to as 'attine ants') represent a classic example of mutualism and coevolution. They comprise a monophyletic group of 248 described species and an additional 31 subspecies in 20 genera (Bolton 2021), all of which cultivate fungus gardens (order Agaricales: families Agaricaceae and Pterulaceae) that they use for food (Wheeler 1907; Weber 1966, 1982; Mueller et al. 1998; Mehdiabadi and Schultz 2010). Attine ants include the leaf-cutting ants, a group of highly derived fungus-farming ant species, which are some of the most ecologically successful species in terrestrial ecosystems. Leaf-cutting ants are very well known in the Americas due to their striking effect on vegetation, especially within human agricultural systems (Lugo et al. 1973), and their impressively large nests (Moreira et al. 2004). In contrast, non-leaf-cutting 'lower' fungus-farming ants are a less conspicuous group that use fallen plant material, feces, or insect pieces as substrates for fungus cultivation (Leal and Oliveira 2000, Mehdiabadi and Schultz 2010, Ronque et al. 2019). Although the study of lower fungus-farming ants is crucial for understanding the origin and evolution of agriculture in ants (Mueller et al. 1998),

they have received less attention than the more derived higher-attine ants. This lack of study is due, in part, to the inconspicuous and small-sized colonies of lower-attine ants and to their negligible impact on human agriculture. Nonetheless, significant contributions to the natural history and evolution of lower fungus-farming ants have been published during the past few decades, including the general biology of *Apterostigma megacephala* Lattke, the only lower-attine ant known to cultivate a higher-attine fungus (Schultz et al. 2015, Sosa-Calvo et al. 2017a); the descriptions of three new genera (Brandão and Mayhé-Nunes 2001, Klingenberg and Brandão 2009, Sosa-Calvo et al. 2013), with implications for the early evolution of agriculture in ants and for the transition to higher agriculture; and the general biology, including nest architecture and the identities of the fungal cultivars, of recently discovered or rare species (Diehl-Fleig and Diehl 2007; Klingenberg et al. 2007; Rabeling et al. 2007; Ješovnik et al. 2013, 2018; Schultz et al. 2015; Sosa-Calvo et al. 2013, 2017a,b).

To date, the genus *Paramycetophylax* Kusnezov remains noteworthy as the only fungus-farming ant genus about which little is known regarding general biology and phylogenetic position (Schultz and Brady 2008, Branstetter et al. 2017a, Li et al. 2018). The genus *Paramycetophylax* was established by Kusnezov (1956) to accommodate the species *Sericomyrmex bruchi* (Santschi 1916). The genus was later synonymized under *Mycetophylax* Emery by Weber (1958), who pointed out morphological similarities shared by *S. bruchi* and *M. cristulatus* (Santschi). In a taxonomic revision of the genus *Mycetophylax*, Klingenberg and Brandão (2009) synonymized *M. cristulatus* (and other subspecies and varieties) under *M. bruchi* and revived the genus *Paramycetophylax* to accommodate *M. bruchi*, thereby disassociating it from the remaining members of *Mycetophylax*, *M. conformis* (Mayr), *M. morschi* (Emery), and *M. simplex* (Emery), as well as from the newly established genus *Kalathomyrmex* Klingenberg and Brandão, containing the single species *K. emeryi* (Forel) (formerly *M. emeryi*). Based on morphology, the phylogenetic position of *Paramycetophylax bruchi* remains enigmatic, explaining why it is placed in its own monotypic genus (Klingenberg and Brandão 2009). Recently, Branstetter et al. (2017a) were able to amplify UCEs from a poorly preserved specimen but, due to its degraded DNA, only a few loci were obtained. Based on the tentative evidence of those loci, *Paramycetophylax* was hypothesized to have arisen somewhere near the base of the genus *Cyphomyrmex* Mayr, which includes the yeast-farming ants (Branstetter et al. 2017a), suggesting that the study of this species could be critically informative about the origin of yeast cultivation, one of the major transitions in the evolution of agriculture in ants (Schultz and Brady 2008). *Paramycetophylax bruchi* is only known to occur in dry habitats in Argentina, having been reported from at least eight provinces (Cuezzo 1998). A reasonably large number of specimens reside in entomological collections in various museums; however, nests have never been excavated and the fungal symbiont thus far remains unknown. Bucher (1974) recorded a short description of nest entrances and subterranean nest architecture that he stated were shared by both *P. bruchi* and *Kalathomyrmex emeryi* colonies. However, as we detail below, these two species have very different nest architectures and Bucher's descriptions, including his record of fungus garden chambers 60 cm below the surface and a large mound of excavated soil at nest entrances, are consistent with colonies of *K. emeryi*. Hence, in this study, for the first time, we (i) document *P. bruchi* nest architecture and colony size based on two colonies collected in the Dry Chaco (Parque Nacional Sierra de las Quijadas, San Luis) and Monte desert (Reserva de Biósfera Ñacuñan, Mendoza) ecoregions in Argentina, (ii) report the phylogenetic position of *P. bruchi* within the Attina by generating new DNA sequences and conducting phylogenomic analyses, and (iii) report the identity of the fungal cultivar of *P. bruchi* and the agricultural system to which it belongs, based on *ITS* 'fungal barcode' molecular data.

Materials and Methods

Study Site

Field work was conducted in the summer during March of 2019 in Parque Nacional Sierra de las Quijadas (PNSQ) at 702 m and during January of 2020 in Reserva de Biósfera Ñacuñan (RBÑ) at 538 m. The PNSQ (S32.46894, W66.96153), located in San Luis Province, protects a transitional area between the Chaco and Monte biogeographic regions. Mean annual precipitation in PNSQ is 250 mm. Dry season occurs from late April to early October and wet season from late October to early April (Cabrera and Willink 1980). In contrast, RBÑ (S34.04535, W67.90742) is located in the Mendoza Province in the central portion of the Monte desert (Karlin et al. 2017). The climate is semiarid and strongly seasonal, characterized by hot, humid summers and dry, cold winters. Mean annual precipitation in RBÑ is 338 mm (based on available records from years 1972 to 2000), very variable between years. Seventy-five percent of the annual rainfall occurs in spring and summer (October–March; Ojeda et al. 1998). Additionally, a *P. bruchi* colony was discovered in El Borbollón, Mendoza (see other examined material). The Reserva Nacional Pizarro (Salta province), located in a transitional area between Yungas Forest and Dry Chaco, was also investigated but no *P. bruchi* populations were found there.

Nest Location and Excavation

The use of Cream of Rice cereal (B&G Foods, Inc., Parsippany, NJ) as a bait, generally useful in attine field studies (Sosa-Calvo et al. 2015), was ineffective for locating foragers of *P. bruchi*. Instead, individual foragers were located by visually searching the surface of the ground. Workers were then followed to their nests and nest entrances were located and marked. We identified the specimens to species using the taxonomic key of Klingenberg and Brandão (2009). From the eight located colonies (six from PNSQ, one from RBÑ, and one from El Borbollón), two entire nests were excavated (one from PNSQ and one from RBÑ) by digging a trench (1.5–2 m deep) ~0.7 m away from the nest entrance and by slowly shaving the soil wall towards the nest entrance until the nest chambers were discovered. Nest architecture was recorded, photographed, and measured following Sosa-Calvo et al. (2015). Ants were collected with flame-sterilized soft forceps and with an aspirator, and fungal cultivar was collected with a flame-sterilized spoon and carefully put into a plastic container. Samples of both the ants and the cultivar were placed into 96% ethanol and RNA*Later* (Invitrogen, ThermoFisher Scientific). Nest chamber dimensions were recorded, including: height (maximum length along the vertical axis), width (maximum length along the horizontal axis parallel to the excavation plane), depth (maximum length along the horizontal axis perpendicular to the excavation plane), and distance from the surface to the chamber floor. A summary of the measurements is presented in Table 1. Fungal and ant vouchers are deposited in the entomological collection of the Museo Argentino de Ciencias Naturales 'Bernardino Rivadavia' in Buenos Aires, Argentina.

Material Examined

In addition to the material collected for this study, we examined other material to study the distribution of this species (Figs. 1 and 2).

Table 1. Nest measurements of the two excavated colonies of *Paramycetophylax bruchi*, including depths and dimensions of individual chambers, chamber contents, and number of individuals

Nest ID	Locality	Date	Chamber	Depth (cm)	Chamber dimensions (cm)			Field notes	Colony size
					Height	Width	Depth		
PNSQPEH2	PNSQ	20.III.2019	1	158.5	1	2	2.5	Fungus garden, larva, dealate queen and workers	120 workers, 9 alate queens, 8 pupae, 1 larva, and 1 dealate queen.
			2	163	2.7	5.5	3	Fungus garden, pupae, alate queens and workers	
PEH1814	RBÑ	11.I.2020	1	123	2.5	4	4	Fungus garden and workers	67 workers and 1 larva
			2	133	2	3.5	2	Fungus garden and workers	
			3	138	2	3	3.5	Fungus garden and workers	
			4	138	2	3	2.5	Fungus garden and workers	
			5	143	2.5	2	4	Fungus garden and workers	

Fig. 1. Automontage images of the worker (left and center columns) and the queen (left column) of *Paramycetophylax bruchi*. (A–C) Lateral view; (D–F) dorsal view; (G–I) full-face view; and (J–L) label information.

Inferred locality information (due to missing GPS coordinates or incomplete locality names on the labels) appears between brackets []. Geographical coordinates were estimated using Google Earth. This material includes:

ARGENTINA. Mendoza: [*Las heras*], [*El*] *Borbollón*, [S32.81215 W68.76573, 675 m], (no collector data), 04.XII.1950, 9 workers, (IFML); MACN_En27824, same as previous entry, but S32.812153 W68.765717, 691 m, (P. E. Hanisch coll.), 30.V.2018, 1 worker (MACN); [*Santa Rosa*], *Reserva de Biósfera Ñacuñan*, [S34.04502 W67.90953, 565 m], (S. Lagos coll.), 13.IX.1997, 4 workers (IADIZA); same as previous entry, but (S. Claver coll.), 26.V.1982, 2 workers (IADIZA); same as previous entry, but 04.XI.1999, 7 workers (IADIZA); same as previous entry, but (G. Debandi coll.), XII.1995, 9 workers, 2 queens (IADIZA); *Santa Rosa*, *El Divisadero*, [S33.75000, W67.68333, 506 m], (M. Rosi and M. Cona coll.), 23.X.2004, 6 workers (IADIZA); same as previous entry, but 17.V.2004, 2 workers (IADIZA); same as previous entry, but 18.V.2004, 4 workers (IADIZA); *Lavalle*, *Reserva* [*provincial*] *Telteca*, [S32.38991 W68.02569, 562 m], (S. Roig and G. Flores coll.), 14.V.1995, 1 worker (IADIZA); same as previous entry, but 19.VII.1996, 1 worker, 1 queen (IADIZA); same as previous entry, but 24.IX.1996, 1 queen (IADIZA); same as previous entry, but S32.385 W68.06083, 13.IIX.1995, 1 queen (IADIZA); same as previous entry, but (G. Flores coll.), 14.VI.1996, 1 queen (IADIZA); same as previous entry, but (G. Debandi coll.), III.1997, 3 workers, 4 queens; **San Juan:** MACN_En27823, *Reserva de Uso Múltiple de Valle Fértil*, S30.72 W67.43, 834m, (A. Saint Esteven, I. Soto, and E. Soto coll.), Pitfall, 3-7.III.2017, 1 worker (MACN). **Salta:** *Anta*, [S24.727730 W64.195655, 476 m], (Luna coll.), VI.1948, 15 workers (IFML). **La Rioja:** [*Independencia*], *Guayapa*, [S30.10555 W66.97666, 501 m], (no collector data), 15.VIII.1948, 2 workers 1 queen (IFML).

IFML: Instituto y Fundación Miguel Lillo, Tucumán, Argentina
IADIZA: Instituto Argentino de Investigaciones de Zonas Áridas, Mendoza, Argentina
MACN: Museo Argentino de Ciencias Naturales 'Bernardino Rivadavia,' Buenos Aires, Argentina

Ant and Fungal DNA Extraction

Ant DNA was extracted using the Qiagen DNeasy Blood and Tissue Kit (Qiagen, Valencia, CA). DNA extractions were performed nondestructively by opening small holes on the right side of the specimen, especially on the pronotum and propodeum, with a sterilized entomological pin to facilitate the lysis process. Cell lysis was performed overnight with 20 µl of Proteinase-K in a dry bath shaker at 56°C and at 500 rpm. We followed the recommendations of the manufacturer for the extraction process except that we eluted the cleaned, extracted DNA from the spin-collection columns with two (rather than one) washes, each consisting of 65 µl of nuclease-free water, differing from the manufacturer's recommendation of 200 µl of AE buffer.

After DNA was extracted, the specimen was washed with 95% ethanol, point-mounted, and properly labelled in order to serve as a voucher specimen in future taxonomic studies (Supp Table 1 [online only]).

Fungal DNA was extracted using the Qiagen DNeasy Plant Mini Kit (Qiagen, Valencia, CA). Fungal tissue was carefully removed from the substrate and placed in a 2 ml tube. Samples were placed in a SpeedVac for 10–15 min at 45°C to remove any ethanol present. Cell lysis was performed overnight in a dry bath shaker at 65°C and at 500 rpm. Elution of the cleaned, extracted DNA from the spin columns was conducted with two steps of 50 µl of AE buffer, as suggested by the manufacturer.

Ant and fungal DNA extractions were quantified using 2 µl samples of DNA template in a Qubit 3.0 Fluorometer and with the High Sensitivity Kit (Thermo Fisher Scientific, Inc.).

Generation of UCE Data

Library Preparation

Before library preparation, 50 ng of DNA template was sheared to an average fragment length of 300–600 bp using a Qsonica Q800R2 Sonicator (Qsonica LLC, Newton, CT) for 60 s. Libraries were prepared in 1.5 ml tubes on a rare magnet stand using the Kapa Hyper Prep Library Kit (Kapa Biosystems, Wilmington, MA) as described in Faircloth et al. (2015) with the iTru Adapter protocol. We implemented all magnetic bead clean-up steps (Fisher et al. 2011) as described in Faircloth et al. (2015) and used dual-indexing TruSeq adapters (Faircloth and Glenn 2012, Glenn et al. 2019) for ligation. The ligation step was followed by PCR-amplification of 15 µl of the library product using 25 µl of KAPA HiFi ReadyMix (Kapa Biosystems, Wilmington, MA), 2.5 µl of each of Illumina TruSeq (i5 and i7) primers, and 5 µl nuclease-free ddH_2O. The following thermal cycler program was executed: 98°C for 45 s; 13 cycles of 98°C for 15 s, 60°C for 30 s, 72°C for 60 s; and final extension at 72°C for 5 m. Following PCR, we purified DNA products using 1.2× Kapa Pure beads and rehydrated the purified product in 22 µl of Elution Buffer (pH = 8). Individual libraries were quantified using 2 µl of library product in a Qubit 3.0 Fluorometer using the Broad Range Kit (Thermo Fisher Scientific, Inc.).

Sample Pooling and Target Enrichment of Libraries

Post-PCR libraries were pooled at equimolar concentrations into one pool containing the ant libraries. Pool concentration was adjusted to 71.5 ng/µl by drying the sample in a vacuum centrifuge for 45–60 min or until all liquid was evaporated at 60°C, and then by resuspending the pool in nuclease-free water at the estimated value. We then used 2 µl of the resuspended product to measure the pool concentration in a Qubit 3.0 Fluorometer with the Broad Range Kit. The final concentration of the preenrichment pool was 78.3 ng/µl.

The pool was enriched by using the ant-customized bait set ('ant-specific-hym-v2') targeting 2,524 conserved loci in Hymenoptera (Branstetter et al. 2017b) at an incubation temperature of 65°C for 24 hr in a thermal cycler. Enrichment, bead-cleaning, and PCR reaction procedures partially followed the Arbor Biosciences v4.0.1 (https://arborbiosci.com/mybaits-manual/) protocol, Borowiec (2019a), and Branstetter et al. (2021). The resulting reaction was purified using 1.0× Kapa Pure beads and the enriched pool was then rehydrated in 22 µl EB. Following this step, the pool was quantified using 2 µl of the enriched pool in a Qubit 3.0 Fluorometer with the Broad Range Kit. To obtain reliable estimates of DNA concentration for the enriched pool, we performed a quantitative qPCR on a ViiA7 Real-Time PCR System (Thermo Fisher Scientific, Inc.) using the KAPA Library Quantification Kit (Kapa Biosystems, Inc) with the KAPA SYBR FAST qPCR Master Mix, universal Illumina primers, and dilutions of 1:1,000,000 and 1:2,000,000. The final enriched pool of 100 µl was submitted to the Laboratories for Analytical Biology (LAB) of the Smithsonian Institution National Museum of Natural History for quality control and sequencing on an Illumina MiSeq (employing the V3 600 MiSeq Kit). New raw sequences generated as part of this study are deposited in the NCBI Sequence Read Archive (SRA; BioProject ID PRJNA771174, BioSample accession numbers SAMN22253136–SAMN22253138).

Amplification and Sequencing of ITS Marker for Fungal DNA

We followed the methods of Mueller et al. (1998) for amplifying and sequencing the nuclear ribosomal internal transcribed spacer (*ITS*) region employing Sanger sequencing. A list of the primers employed for *ITS* amplification can be found in Sosa-Calvo et al. (2019). Sequencing was performed in the Laboratories for Analytical Biology (LAB) of the Smithsonian Institution National Museum of Natural History on an ABI 3100 automated sequencer using an ABI BigDye Terminator v3.1 Cycle Sequencing Kit (Applied Biosystems Inc., Foster City, CA). Sequence data were assembled and edited using the program Sequencher v.4.10.1 (Gene Codes Corp., Ann Arbor, MI).

To determine the identity of the fungal cultivar grown by *Paramycetophylax bruchi*, we added its *ITS* sequence to a large *ITS* alignment (304 taxa and 1017 characters) that includes both free-living fungal sequences and ant-associated fungal sequences (Mueller et al. 1998; Vo et al. 2009; Mehdiabadi et al. 2012; Schultz et al. 2015; Sosa-Calvo et al. 2017b, 2019; Sosa-Calvo and Schultz, unpublished data). The new ITS sequence of *Paramycetophylax bruchi* generated for this study is deposited in GenBank under accession number OK569851.

Molecular Phylogenetics

Processing of UCE Sequence Data

The ant phylogenomic analyses are based on a modified version of the alignments used in Branstetter et al. (2017a) and Li et al. (2018), into which we incorporated new sequences belonging to three colonies (representing two populations) of the fungus-farming ant species *Paramycetophylax bruchi* and trimmed reads from eight taxa belonging to the tribe Crematogastrini generated for the study of Blaimer et al. (2018) that we downloaded from NCBI Sequence Read Archive.

For the newly generated *P. bruchi* sequences, we trimmed the demultiplexed FASTQ output files generated by the Smithsonian Institution National Museum of Natural History's Laboratory of Analytical Biology for adapter contamination and low-quality bases using Illumiprocessor v.2.0.6 (Faircloth 2013), which includes Trimmomatic v0.39 (Bolger et al. 2014). We used SPAdes v.3.14 (Bankvich et al. 2012, Nurk et al. 2013) for the assembly of reads into contigs. We relied on a series of scripts available in the PHYLUCE package (Faircloth 2016) to further process our data and we followed the methods used in Branstetter et al. (2017a), Ješovnik et al. (2017), and Li et al. (2018).

We aligned each UCE locus using MAFFT v7.407 (Katoh and Standley 2013) using the default algorithm, then we aligned each locus again using the L-INS-i algorithm, which tends to generate more accurate alignments (Katoh et al. 2005, Katoh and Standley 2014). We trimmed poorly aligned regions in each UCE locus with GBLOCKS (Castresana 2000, Talavera and Castresana 2007) using relaxed settings (b1 = 0.5, b2 = 0.5, b3 = 12, b4 = 7). An initial alignment was generated by first aligning individual UCE loci with at least 98 taxa represented (70% completeness) using the PHYLUCE script *phyluce_align_get_only_loci_with_min_taxa*. We then concatenated those loci into a data matrix using the PHYLUCE script *phyluce_align_format_nexus_files_for_raxml*, named Pbruchi_70p, for downstream analyses. The resulting data matrix consisted of 136 taxa (57 outgroup taxa and 79 fungus-farming-ant taxa) and 558,222 nucleotide characters representing 942 UCE loci.

UCE Phylogenetic Analyses

Initial analyses were conducted on the unpartitioned Pbruchi_70p alignment using IQTREE multicore v.2.0.6 (Minh et al. 2020), the GTR+F+G4 model of evolution (as selected by IQTREE), the default number of unsuccessful iterations to stop (-nstop 100), and an initial neighbor-joining tree (-t BIONJ). Node support was estimated by conducting 2,000 ultrafast bootstraps (UFBoot; Hoang et al. 2018).

To identify and remove outlier or poorly aligned sequence fragments we used the Python tool SPRUCEUP (Borowiec 2019b) on the Pbruchi_70p dataset. We set the parameters in the configuration file to the uncorrected p-distance for computing the distances, a window size of 20 bp with an overlap of 15 bp, a lognormal distribution to identify outlier distances, and a global cutoff of 0.95. As a result, SPRUCEUP changed 268,450 (0.35%) outlier nucleotide-site state assignments (i.e., matrix cell values) to gaps (Supp Table 3 [online only]). We then used the SPRUCEUP-trimmed alignment and repeated the unpartitioned analysis using the same parameters as above, including 1,000 replicates of the SH-like approximation likelihood-ratio test (-alrt 1000; Guindon et al. 2010).

Using the same trimmed alignment, we conducted three different partition tests: (i) By-locus partitions, in which each UCE locus is a partition (942 total) and in which each partition is given the same model (GTR+G+F4). (ii) Best scheme by locus, in which ModelFinder (Kalyaanamoorthy et al. 2017), as implemented in IQTREE (Minh et al. 2020), is used to identify the best partitioning scheme by allowing two or more UCE loci to be merged into partitions and to identify the best-fitting models. For the merging step, we used the *-m MF+MERGE* commandm, the fast relaxed *-rclusterf* algorithm (set to 10; Lanfear et al. 2017) and compared the top 10% of the resulting partitioning schemes using the corrected Akaike information criterion (AICc), restricting the evaluated models to those implemented in RaxML by using the command *-mset raxml*. The best-fit partitioning scheme (Pbruchi_70p_trimmed_bestscheme_bylocus) consisted of 484 subsets. (iii) The Sliding Window Site Characteristics based in Entropy method (SWSC-EN; Tagliacollo and Lanfear 2018), in which each UCE locus is split into three regions (a core and two flanking regions). The SWSC-EN algorithm identified 2,826 subsets. We then identified the best partitioning scheme by merging the resulting subsets using ModelFinder (Kalyaanamoorthy et al. 2017) as implemented in IQTREE (Minh et al. 2020), employing the same merging steps as in the partitioning scheme (ii) above. The best-fit partitioning scheme (Pbruchi_70p_trimmed_SWSC-EN) consisted of 853 subsets (see Supp Table 5 [online only]).

We performed further maximum-likelihood (ML) analyses on the trimmed alignment with the different partitioning schemes using IQ-TREE multicore v.2.0.6 (Chernomor et al. 2016, Minh et al. 2020), estimating branch support with the ultrafast bootstrap (Hoang et al. 2018) and the SH-like approximation likelihood ratio test (Guindon et al. 2010) set at 1,000 replicates, with other settings set at default values. Maximum-likelihood analyses of the unpartitioned dataset, the trimmed dataset, and of datasets under the three different partitioning schemes listed above indicate that the results of the trimmed SWSC-EN partitioned dataset have a better log-likelihood score than the alternatives (SWSC-EN = −8,045,748.129; Best scheme by Locus = −8,124,383.749; By Locus = −8,140,819.136; trimmed unpartitioned = −8,195,808.463; unpartitioned = −8,799,158.824).

We conducted matched-pair tests of symmetry (Naser-Khdour et al. 2019) as implemented in IQ-TREE v.2.1.2 (Chernomor et al. 2016, Minh et al. 2020) to test model violation by testing assumptions of stationarity and homogeneity. To remove the bad partitions, we employed the *--symtest-remove-bad* option and set the *P*-value cutoff as the default ($P = 0.05$). A total of 67/853 partitions were removed from the SWSC-EN partition scheme, 124/942 partitions were removed from the by-locus partition scheme, and 84/484 partitions

were removed from the merged-by-locus scheme. The resulting 'good' partitions and 'good' alignments were then used to generate new ML analyses in IQTREE, which resulted in the trees in Supp Fig. 1 [online only] with the following log-likelihood scores: SWSC-EN-symtest = −7,231,029.242, by-locus-symtest = −7,027,206.003, and merged-by-locus-symtest = −6,534,146.568.

Divergence-Dating Inference

To estimate the time of divergence of the genus *Paramycetophylax* and its sole species *P. bruchi* from its sister group, we used the Bayesian program MCMCTREE (Yang and Rannala 1997), implemented as part of the PAML package (Yang 2007), which uses the approximate-likelihood approach of Thorne et al. (1998). We input the SPRUCEUP-trimmed alignment and the topology generated using the SWSC-EN and ModelFinder best-fitting models. To calibrate our analysis, we employed information available from two fossils as well as from two published studies (as secondary calibrations). The two fossils were: (i) A *Pheidole* Westwood species from the Florissant Formation (34 Ma; Carpenter 1930, Ward et al. 2015), calibrating the crown node of the genus *Pheidole* and modeled as the Cauchy distribution L (0.34, 0.05, 0.085, 1e-300). (ii) *Mycetomoellerius primaevus* (Baroni Urbani) from Dominican Amber (15 mya; Baroni-Urbani 1980), calibrating the most-recent common ancestor (MRCA) of *Mycetomoellerius* Solomon et al. and *Acromyrmex* Mayr, i.e., the higher Attina, and modeled as the uniform distribution B (0.15, 0.35), i.e., of 15 mya to 35 mya (Supp Table 4 [online only]). In a recent phylogenetic study in which the genus *Trachymyrmex* s.l. was divided into three monophyletic genera (Solomon et al. 2019), the species '*Trachymyrmex*' *primaevus* was tentatively placed in the genus *Mycetomoellerius* (Solomon et al. 2019). Because there remains significant uncertainty about the phylogenetic position of this fossil (Schultz and Sosa-Calvo, personal observation), we used it to conservatively calibrate the MRCA of the higher Attina (*Mycetomoellerius* + *Acromyrmex*, Schultz and Brady 2008, Branstetter et al. 2017a, Li et al. 2018) rather than the crown node of *Mycetomoellerius*. The two secondary calibrations were: (i) The crown age of the subfamily Myrmicinae (95% CI 110.1 mya to 87.1 mya, median 98.6 mya; Ward et al. 2015, Branstetter et al. 2017a), modeled as the skew-normal distribution SN (0.986, 0.06, 0) using the R package MCMCtreeR (Puttick 2019). (ii) The crown age of the tribe Crematogastrini (95% CI 93.704 mya to 66.132 mya, median 78.55 mya; Blaimer et al. 2018) modeled as the skew-normal distribution SN (0.7855, 0.08, 0; Supp Table 4 [online only]). For each of the skew-normal distributions, we note that the shape parameter (third term) is zero, creating a symmetrical distribution around the median age (first term). The number of calibrations used in our analysis, four, differs from the number of calibrations (ten) employed in the study of Branstetter et al. (2017a) for three reasons: (i) to avoid potentially misidentified fossils (affecting one calibration, that of the Stenammini); (ii) to avoid conflict across calibrations (affecting one calibration, that of *Myrmica* Latreille + *Manica* Jurine); and (iii) to avoid calibrations lacking information content, i.e., calibrations based on Dominican amber fossils (15 mya) for taxa that are clearly much older (affecting four taxa).

MCMCTREE analyses used the independent-rates clock model and the GTR+G4 substitution model. We conducted four independent MCMCTREE runs, each consisting of 50 million generations, and each with the following settings: sampfreq = 1,000, nsample = 50,000, and burnin = 5,000,000. We assessed run convergence and stationarity by examining the resulting mcmc.txt files in Tracer v1.7.1 (Rambaut et al. 2018) using the criterion of ESS values higher than 500. Analyses were conducted on the Smithsonian High Performance Cluster (SI/HPC), Smithsonian Institution (https://doi.org/10.25572/SIHPC).

Fungi

ITS Sequencing and Phylogenetics

DNA sequences of the fungal cultivar of *Paramycetophylax bruchi* were incorporated into a large *ITS* alignment (305 sequences) including both attine fungal cultivars and free-living Agaricales fungi generated during the past 15 years (Mueller et al. 1998, Vo et al. 2009, Mehdiabadi et al. 2012, Sosa-Calvo and Schultz, unpublished data). We aligned the fungal dataset using the online version of MAFFT v7 (Katoh et al. 2019). The resulting alignment was submitted to the guide-tree-based GUIDANCE2 server (Sela et al. 2015) to identify poorly aligned sites to be masked (excluded) from further analysis. The final *ITS* alignment included 1,017 aligned sites, including indels, and 561 parsimony-informative sites. We divided the alignment into two blocks (*ITS*fast and *ITS*slow) based on site variability, as in Mehdiabadi et al. (2012) and Masiulionis et al. (2014). We performed Bayesian analyses using MrBayes v.3.2.7a (Ronquist et al. 2012) in the CIPRES Science Gateway (Miller et al. 2010). The analysis consisted of two runs and eight chains, with a sampling frequency of 1,000 and 10,000,000 generations, and with burn-in set at 1,000,000. We set the parameter brlenspr = unconstrained:Exp(100) due to known problems with estimation of branch lengths in MrBayes (Marshall et al. 2006, Brown et al. 2010, Marshall 2010). We assessed burn-in, convergence, and stationarity by using the program TRACER v.1.7.1 (Rambaut et al. 2018).

Results

Natural History

Habitat

Based on data associated with the examined material and the type localities, specimens of *Paramycetophylax bruchi* have been collected from low to high elevations (50–2069 m) in the Dry Chaco and Monte ecoregions in Argentina (Fig. 2; Klingenberg and Brandão 2009). We collected this species from both ecoregions at three localities (PNSQ, RBÑ, and El Borbollón) from mid to high elevations (538–702 m). PNSQ and RBÑ sites have in common a high density of the tree *Prosopis flexuosa* De Candolle (Fabaceae), locally known as Algarrobo dulce (Alvarez and Villagra 2009). Populations of this tree species were also present in two other localities (El Borbollón, Mendoza, and Reserva de Uso Múltiple de Valle Fértil, San Juan; Hanisch and Saint Esteven, personal observation; see material examined). Moreover, all the located colonies (n = 8) were found under the canopy of this tree species (Fig. 3A–C). Our field observations indicate that workers of *Paramycetophylax bruchi* forage individually throughout the day for substrate near the colony (n = 7). In one case (RBÑ colony) the ants were only seen active at night removing dry leaves (presumably used-up garden substrate) from the nest. All foraging individuals observed were carrying *Pr. flexuosa* leaflets (Fig. 3D). Typically, foragers left the leaflets inside the nest entrance and departed to look for another leaflet.

Nest Architecture

Nest entrances of *Paramycetophylax bruchi* consisted of a single inconspicuous hole in the ground (3–4 mm in diameter), sometimes with a shallow mound of excavated soil a few centimeters away from the entrance (Fig. 4A–C). In no case was the nest entrance located at the top of the excavated soil, differing in this regard from some of the colony

Fig. 2. Known distribution of *Paramycetophylax bruchi*. Type locality (black star) and type localities of three synonymized subspecies and varieties (white stars); our study sites (black dots); and additional sites from examined material (white dots).

entrances of *Kalathomyrmex emeryi* (Bucher 1974; Fig. 4D). Two colonies of *P. bruchi* were excavated (one from PNSQ and one from RBÑ) and censused. Nests consisted of 2–5 chambers located 123–163 cm below the surface. With the exception of the deepest chamber at PNSQ, which was heart-shaped, chambers were elliptically shaped, 2–5.5 cm wide and 1–2.7 cm high. The largest garden chamber encountered (PNSQ, chamber 2) was 2.7 × 5.5 cm. Information regarding nest architecture is summarized in Table 1 and Fig. 5.

Colony Size

The excavated PNSQ colony consisted of 120 workers, 9 alate queens, 8 pupae, 1 larva, and 1 dealate queen. The excavated RBÑ colony consisted of 67 workers and 1 larva. Because no dealate queen was found, the RBÑ colony excavation may have been incomplete, unless we excavated a queenless colony or the queen escaped during the excavation. Based on the many queens found in the material examined in the IADIZA collection, nuptial flights occur from March to December, mostly coinciding with the time of highest rainfall.

Fungal Symbiont

All chambers contained fungus gardens resting on the chamber floor (Fig. 6A), which consisted of leaflets of *Pr. flexuosa* covered with fungal mycelium (Fig. 6B–D).

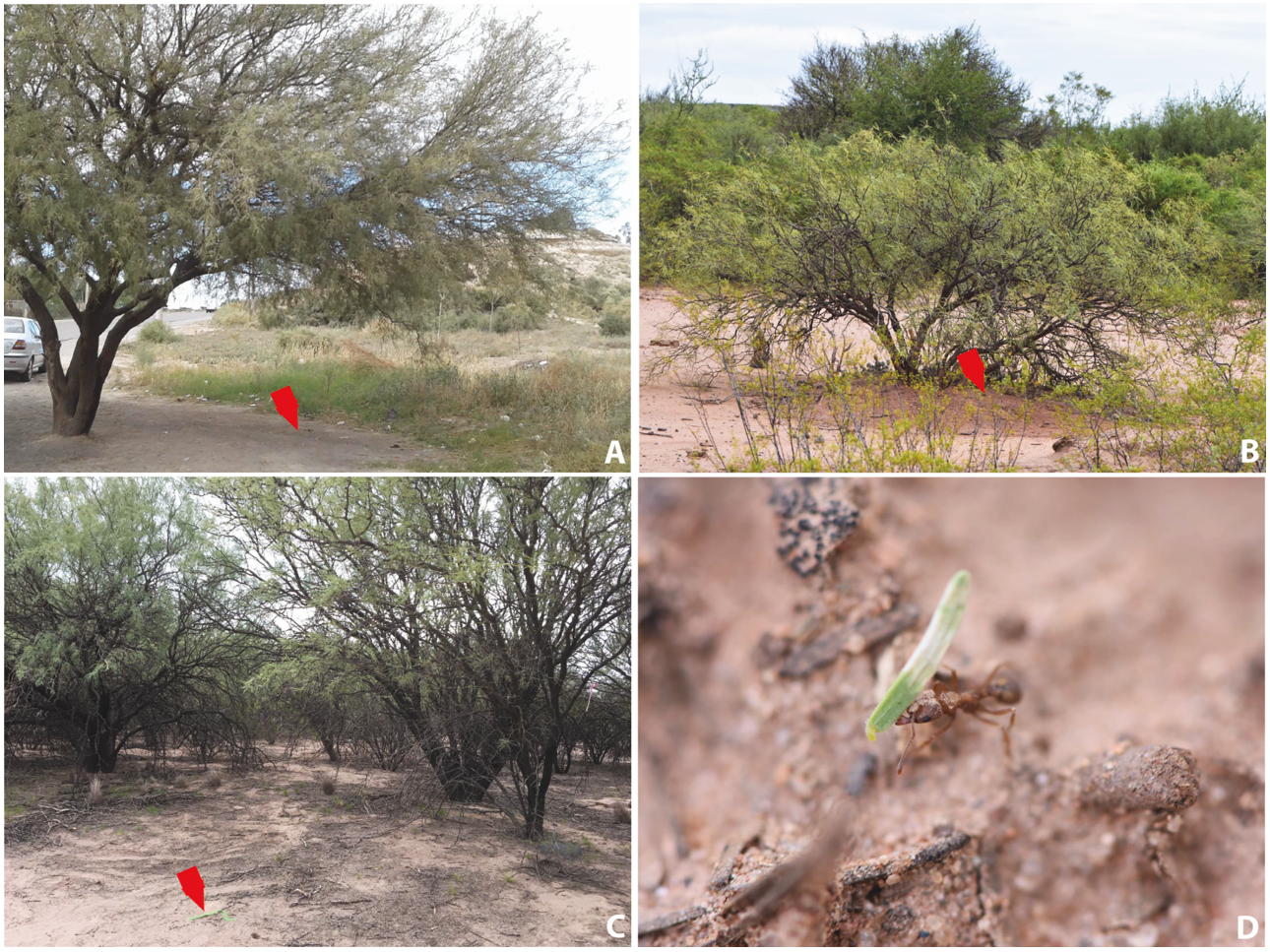

Fig. 3. Habitat of *Paramycetophylax bruchi*. (A) El Borbollón, Mendoza, Argentina; (B) Parque Nacional Sierra de las Quijadas, San Luis, Argentina; and (C) Reserva Biósfera Ñacuñan, Mendoza, Argentina. (D) A forager of *P. bruchi* carrying a *Prosopis flexuosa* leaflet. Red arrows indicate the location of the nest of *Paramycetophylax bruchi*.

Molecular Phylogenetics and Divergence-Dating Analysis

With regard to the relationships of genera and species, our phylogeny (Fig. 7, Supp Fig. 2 [online only]) agrees with previous phylogenomic analyses of the Attina (Branstetter et al. 2017a, Li et al. 2018). As in these previous studies, we also recover with maximum support the monophyly of fungus-farming ants and their sister-group relationship to the informal subtribe 'Dacetina' (the former 'Dacetini' excluding *Strumigenys*; Fig. 7, Supp Figs. 1 and 2 [online only]). Unlike those previous studies, however, our data include newly generated sequences from recently collected specimens of *Paramycetophylax bruchi*. Our partitioned maximum-likelihood analysis indicates, with maximum support, that the genus *Paramycetophylax* is the sister group of the *Cyphomyrmex rimosus* group of yeast-cultivating ant species, arising between the yeast farmers and the mycelium-cultivating *C. wheeleri* group and thus rendering the genus *Cyphomyrmex* paraphyletic (Fig. 7, Supp Figs. 1 and 2 [online only]).

Our Bayesian divergence-dating analysis conducted in the program MCMCTREE (Fig. 8, Supp Figs. 3–7 [online only]) produced slightly older ages compared to those found in Branstetter et al. (2017a) and Li et al. (2018), especially for the Attini, the Attina, and the two, early-diverging, sister clades of fungus-farming ants, the 'Paleoattina' and the 'Neoattina' clades. Our results indicate that the Attini evolved in the Late Cretaceous, 77 Ma (68–87 mya, HPD), with major genus groups evolving very shortly thereafter. The fungus-farming ants originated at the end of the late Cretaceous sometime between 68 mya (59–76 mya; crown) and 73 mya (64–82 mya; stem). The paleoattine and the neoattine clades were recovered as originating 60 mya (51–69 mya) and 59 mya (51–68 mya), respectively. Within the Attina, our analysis recovered dates for the higher attines and leaf-cutters similar to those of previous analyses (Supp Table 6 [online only]). The *Cyphomyrmex* clade, containing the *C. wheeleri* group, the *C. rimosus* group, and the genus *Paramycetophylax*, evolved 37 mya (31–43 mya; crown) in the Late Eocene. The genus *Paramycetophylax* diverged from its sister group, the *C. rimosus* group, very shortly afterward around 36 mya (30–42 mya).

Bayesian analyses of the ribosomal *ITS* 'fungal DNA barcoding' gene fragment indicate that *Paramycetophylax bruchi* practices lower agriculture, i.e., that it cultivates a fungal species that falls within a known group of leucocoprineaceous ant-associated fungi within the family Agaricaceae. More specifically, the fungal cultivar grown by *P. bruchi* belongs to lower-attine 'Clade 1' in the vicinity of Clade 1 subclades 1A and 1B of Mehdiabadi et al. (2012). In the *ITS* phylogeny, this clade also includes fungi cultivated by

Fig. 4. Nest entrances of *Paramycetophylax bruchi* at (A) El Borbollón, Mendoza, Argentina; (B) Parque Nacional Sierra de las Quijadas, San Luis, Argentina; and (C) Reserva Biósfera Ñacuñan, Mendoza, Argentina. (D and inset) Nest entrance from Reserva Nacional Pizarro (Salta) of *Kalathomyrmex emeryi* shown here for comparison.

other members of the genus *Cyphomyrmex* (Fig. 9; e.g., *C. wheeleri* Forel, *C. longiscapus* Weber, *C. costatus* Mann) and a gongylidia-producing *Mycocepurus* Forel cultivar, and it is closely related to the clade of yeast fungi (Mehdiabadi and Schultz 2010, Mehdiabadi et al. 2012, Masiulionis et al. 2014, Sosa-Calvo et al. 2019).

Discussion

During the last three decades, fungus-farming ants have become a model system for the study of symbiotic evolution. As a result, the natural history and evolution of fungus-farming ant species have been the subjects of increasing study. Several new genera have been described (*Amoimyrmex* Cristiano et al.; *Cyatta* Sosa-Calvo et al.; *Kalathomyrmex*, *Mycetagroicus* Brandão, and Mayhé-Nunes; *Mycetomoellerius*, *Paratrachymyrmex* Solomon et al.; *Xerolitor* Sosa-Calvo et al.) as a result of targeted fieldwork and molecular systematics (Brandão and Mayhé-Nunes 2001; Klingenberg and Brandão 2009; Sosa-Calvo et al. 2013, 2018; Solomon et al. 2019; Cristiano et al. 2020). In other cases, species have been transferred between genera in order to maintain taxonomic stability (Sosa-Calvo et al. 2017b). The study of symbiotic evolution and coevolution of the fungus-farming ants and their fungal cultivars has resulted in the recognition of five distinct 'agricultural systems' characterized by more-or-less consistent associations of phylogenetic groups (clades or grades) of ant species with phylogenetic groups of fungal cultivar species (see Schultz and Brady 2008, Mehdiabadi et al. 2012, Schultz et al. 2015, Branstetter et al. 2017a). The origins of these systems represent major transitions in the evolutionary history of ant agriculture (Schultz and Brady 2008).

The genus *Paramycetophylax* is among the most rarely collected of fungus-farming ant genera. As a result, its nesting behavior, colony demography, fungal cultivar(s), and position in the fungus-farming ant tree of life have remained enigmatic. We were able to collect specimens from eight colonies, and to excavate two entire colonies, of the species *Paramycetophylax bruchi*, the sole member of the genus, in Argentina. Our new collections expand the known distribution of this species (Klingenberg and Brandão 2009). The areas where the colonies were collected are classified as dry to arid regions (Bruniard 1982, Brown et al. 2005). Surprisingly, one of the colonies was found in a small town (El Borbollón) and, hence, in a highly disturbed area (Fig. 3A). The nests of this species, like those of several other species of fungus-farming ants, tend to have inconspicuous openings accompanied by some excavated soil near the entrance. Nest chambers were found at depths between 123

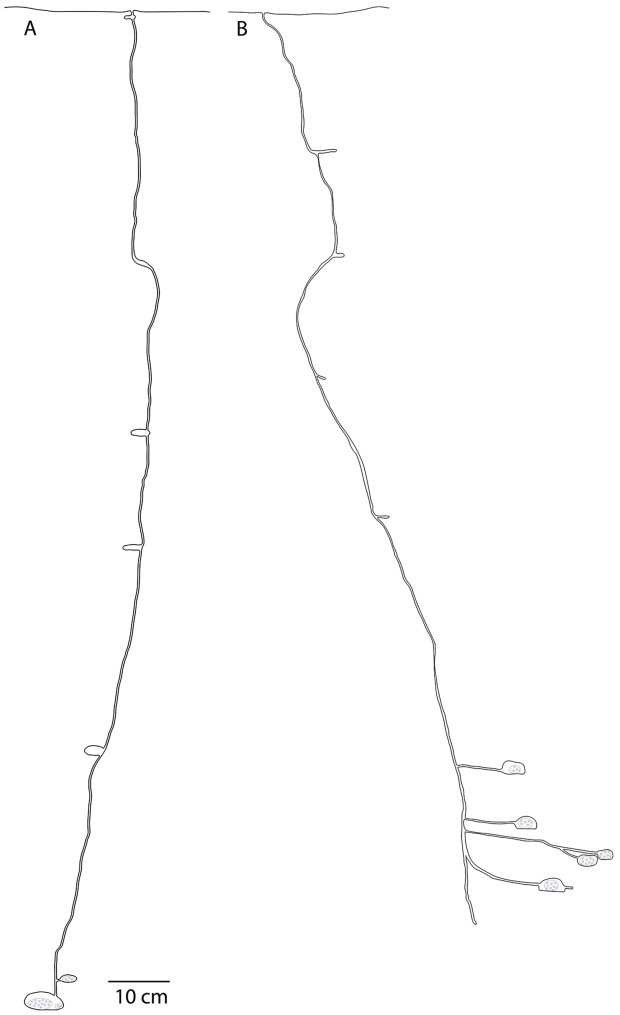

Fig. 5. Illustration of *Paramycetophylax bruchi* nests at (A) Parque Nacional Sierra de las Quijadas, San Luis, Argentina; and (B) Reserva Biósfera Ñacuñan, Mendoza, Argentina.

and 163 cm below the surface. Some other dry-habitat-inhabiting fungus-farming ants (e.g., *Cyatta*, *Mycetagroicus*) excavate nests with a few small chambers that are much deeper than those of *Paramycetophylax* (Solomon et al. 2011, Ješovnik et al. 2013, Sosa-Calvo et al. 2013), whereas others, such as *Xerolitor explicatus* Kempf, which is also found in the Dry Chaco of Paraguay, have slightly shallower nests (Sosa-Calvo et al. 2018). Workers of *P. bruchi* were observed collecting and carrying leaflets of the legume plant *Prosopis flexuosa* (Fabaceae) to their nest (Fig. 3D). These leaflets were used as a substrate for their fungal cultivar, which grows as small patches of mycelium on the intricate leaflet mass (see Fig. 6). A similar leaf-carrying behavior has been observed in the paleoattine ant *Apterostigma megacephala* Lattke in Amazonian wet forest in Brazil, the only lower-attine ant known to cultivate a higher-attine fungus (Schultz et al. 2015, Sosa-Calvo et al. 2017a). Individuals of this species also collect and carry into their nest leaflets of another legume plant, *Pseudopiptadenia suaveolens* (Miquel) (Fabaceae); however, in contrast to the use of *Pr. flexuosa* leaflets by *P. bruchi*, *A. megacephala* does not use *Ps. suaveolens* leaflets as a garden substrate. Instead, the leaflets were observed to serve as a covering for the floor of the garden chamber (Schultz et al. 2015, Sosa-Calvo et al. 2017a). The fact that all colonies of *P. bruchi* were associated with *Pr. flexuosa* is interesting, considering that the distribution of these two species is similar (Alvarez and Villagra 2009, Klingenberg and Brandão 2009, this study). If this correlation is consistent, our results suggest other localities where *P. bruchi* could be found. *Prosopis flexuosa* is an ecologically important species, serving as a major food source for vertebrates and insects, including ants (Milesi and Casenave 2004), and improving soil properties (Rossi and Villagra 2003). As a result, it produces spatial heterogeneity that modifies the species distributions of both plants and animals. Finally, it is important to point out that our data are restricted to a few populations and colonies of *P. bruchi* and therefore likely reflect just a part of its biology. Therefore, the generality of our results should be confirmed by studying more colonies and populations.

Our phylogenetic analysis places *Paramycetophylax* within the genus *Cyphomyrmex* (Fig. 7). As currently circumscribed, *Cyphomyrmex* is phylogenetically divided into two species groups, each of which is distinct with regard to the agricultural system it practices. In the *C. wheeleri* group, all the species grow their cultivars as mycelium, consisting of chains of connected cells, whereas in the *C. rimosus* group, all the species grow their fungal cultivars in a yeast-like phase consisting of small nodules of nonconnected fungal cells. Our maximum-likelihood analysis indicates, with maximum support, that *Paramycetophylax* is the sister group to the *C. rimosus* group, thus rendering the genus *Cyphomyrmex* paraphyletic. In the interest of taxonomic stability, one of three actions is thus required: (i) the genus *Paramycetophylax* must be synonymized under the genus *Cyphomyrmex* as currently defined; (ii) the genus *Paramycetophylax* must be synonymized under a more narrowly circumscribed *Cyphomyrmex* consisting solely of the yeast-cultivating *C. rimosus* species, which includes the type species of *Cyphomyrmex*, and the *C. wheeleri* group must be elevated to the status of a separate genus; or (iii) *Paramycetophylax* must be maintained as a valid genus, the definition of *Cyphomyrmex* must be narrowed to include only the *C. rimosus* group, and the *C. wheeleri* group must be elevated to the status of a separate genus. We have chosen not to undertake any of these actions in this paper because we feel it is more appropriate to do so in the context of a global taxonomic revision of the genus *Cyphomyrmex*, currently underway (Zoppas de Albuquerque et al. in progress).

The ages produced by our divergence-dating analyses for the Attini, the Attina, and the two major clades within the Attina (the 'Paleoattina' and the 'Neoattina') are slightly older than those reported by Branstetter et al (2017a). These older ages likely result from differences between the two analyses, which include (i) we employed a reduced number of calibrations (four rather than ten; see Materials and Methods), and (ii) we included species from the Crematogastrini, a myrmicine tribe not included in the Branstetter et al. (2017a) study, allowing us to make use of a secondary calibration taken from Blaimer et al. (2018). Our taxon sampling of the genus *Pheidole* included *Ph. fimbriata* Roger, the sister group to the remainder of the genus (Moreau et al. 2008; Economo et al. 2015, 2019), which allowed us to calibrate the *Pheidole* crown node based on a fossil from the Florissant Formation (34 Ma). Although it might be argued that the *Pheidole* fossil instead represents a stem taxon, i.e., that it is older than the MRCA of extant *Pheidole* species (Economo et al. 2015), the placement of this fossil is in fact irrelevant to our results. In alternative dating analyses in which we used the fossil to calibrate the stem node (Supp Figs. 4 and 6 [online only]), and in analyses in which we did not include the *Pheidole* calibration at all (Supp Fig. 5 [online only]), we obtained nearly

Fig. 6. Fungus gardens. (A) Subterranean garden chamber at Reserva Biósfera Ñacuñan (RBÑ), Mendoza, Argentina; (B) fungus garden and ants in field nest boxes at Parque Nacional Sierra de las Quijadas, San Luis, Argentina; (C–D) fungus garden and ants in field nest boxes at RBÑ.

identical dating results, indicating that the *Pheidole* fossil calibration contains little information and did not play a role in our discovery of ages slightly older than those found in previous studies (Supp Table 6 [online only]). Our dating analyses indicate that the MRCA of *Paramycetophylax* and the *C. rimosus* group lived around 36 mya (30–40 mya, 95% HPD), coinciding with the Terminal Eocene Event (33.9 mya; Fig. 7, 'TEE'), a period of global cooling during which large portions of South America underwent a change in vegetation from subtropical woodlands to seasonally arid savanna woodlands, and in which the first ice sheets formed in Antarctica and large-scale species turnover occurred globally due primarily to extinctions of tropical-adapted species (Prothero 1994, Zachos et al. 2001). Both sister clades are subtended by long, unbroken branches (29 Myr for *Paramycetophylax*, 20 Myr for the *C. rimosus* group) that indicate long periods of anagenesis and/or extinction. Because *P. bruchi* currently occupies seasonally dry or arid habitats, it is tempting to speculate that it is the sole relict species of a dry-habitat-inhabiting lineage that, after originating during the TEE, remained specialized on dry habitats. In contrast, the 19 extant (and two fossils) species in the *C. rimosus* group are diverse with regard to habitat, abundant in wet forests but also found in dry habitats and at high elevations, ranging from the southern United States to Argentina (Kempf 1965, Snelling and Longino 1992). This pattern of a depauperate dry-habitat-inhabiting lineage as sister to a diverse wet-and-dry-habitat-inhabiting clade occurs elsewhere in the fungus-farming ants, most notably in the split between the lower-attine genus *Mycetagroicus* and the higher Attina (Fig. 8), which also occurred coincident with the TEE.

Our Bayesian phylogenetic analysis of the fungal cultivar of *Paramycetophylax bruchi* (Fig. 9) indicates that *P. bruchi* practices lower agriculture, the likely ancestral condition in fungus-farming ants (Schultz and Brady 2008, Branstetter et al. 2017a), and that its fungal cultivar falls within Clade 1 of the lower-attine fungi (Mueller et al. 1998, Vo et al. 2009, Mehdiabadi et al. 2012), a clade that, interestingly, also includes the yeast fungi cultivated by the *Cyphomyrmex rimosus* group of fungus-farming ants, the sister group of *P. bruchi* (Fig. 7). More definitive phylogenetic analyses of the ant-cultivated fungi, preferably employing phylogenomic markers (e.g., UCEs), are necessary for understanding deeper relationships and species boundaries in the ant-cultivated fungi. Our results clearly indicate that increased studies of *Paramycetophylax bruchi* and of its fungal cultivar, especially analyses of whole genomes compared with those of *C. rimosus*-group ants and fungi, are essential for understanding the origin of the ancestral yeast cultivar from a Clade 1 mycelial ancestor, one of the major transitions in the evolution of agriculture in ants (Schultz and Brady 2008).

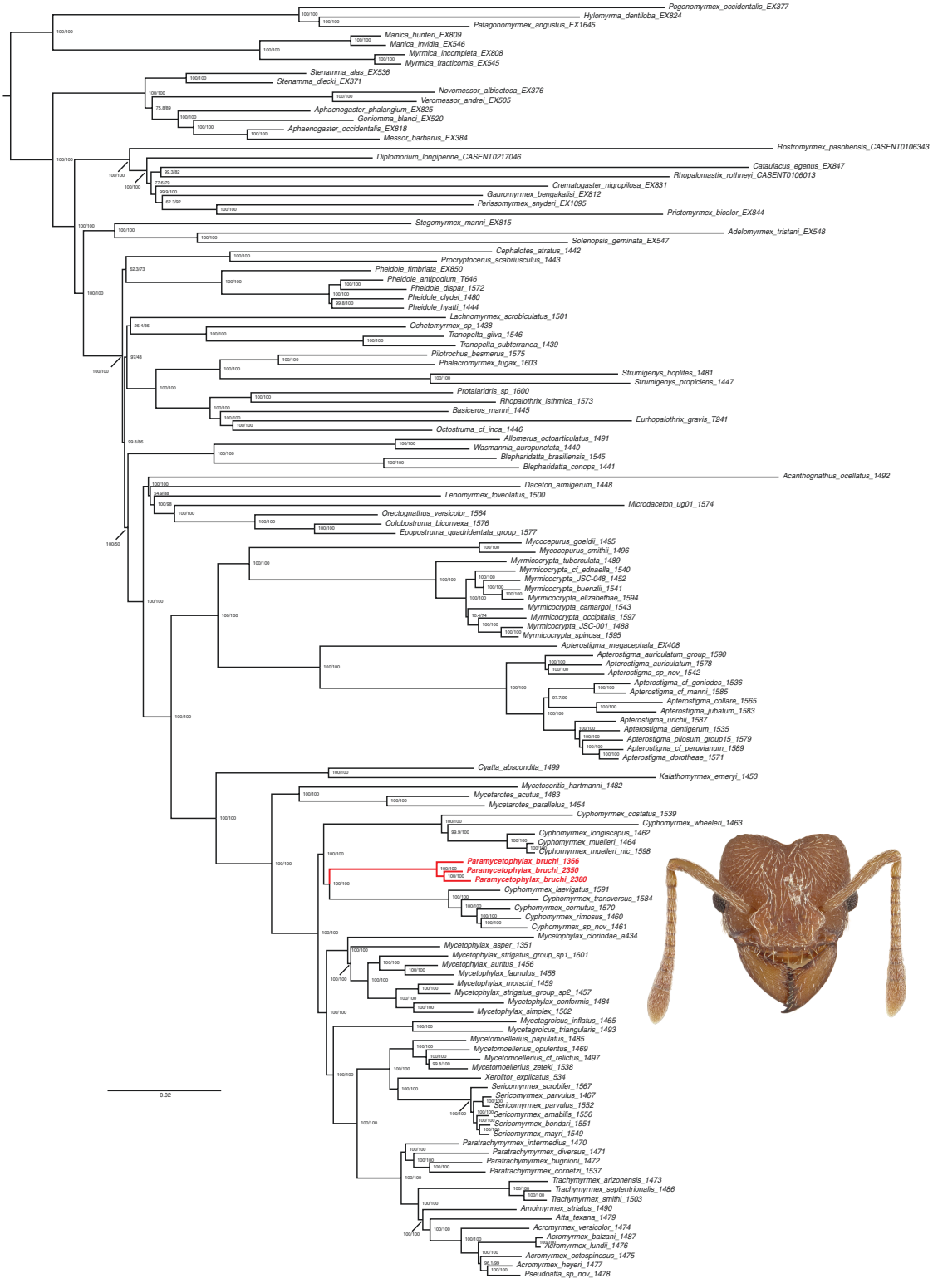

Fig. 7. Phylogeny of the Myrmicinae based on a SWSC-EN partitioned maximum-likelihood analysis in IQTREE (Chernomor et al. 2016, Minh et al. 2020). Support values on branches indicate the SH-like approximation likelihood-ratio test (alrt) and ultrafast bootstrap (UFBoots) proportions, respectively. Red branches indicate the position of *Paramycetophylax bruchi*. Inset: Automontage image of the head of a *P. bruchi* worker.

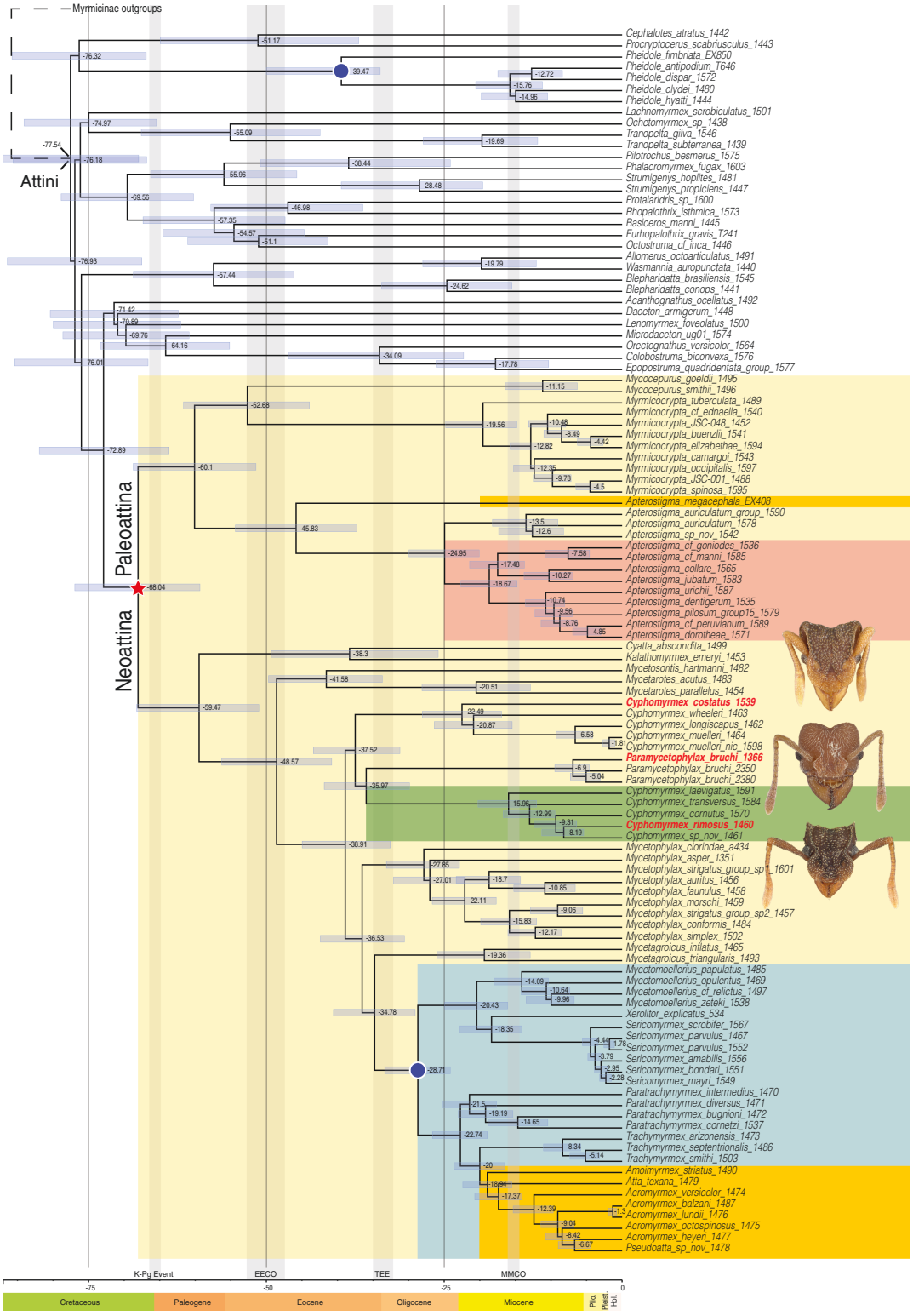

Fig. 8. Time-calibrated phylogeny of the tribe Attini inferred from an MCMCTREE analysis (Yang and Rannala 1997). Red star indicates the origin of fungus-farming ants. Blue dots indicate fossil calibrations (see text). Colored boxes indicate the five agricultural systems: (i) lower agriculture (yellow); (ii) coral-fungus (Pterulaceae) agriculture (red); (iii) yeast agriculture (green); (iv) higher agriculture (blue); and (v) leaf-cutter agriculture (orange). Taxa in red correspond to ant-head images on right: *Cyphomyrmex costatus* (top), *Paramycetophylax bruchi* (middle), and *C. rimosus* (bottom). Light blue bars indicate 95% highest probability density (HPD). K-Pg Event = Cretaceous/Paleogene boundary; EECO = Early Eocence Climatic Optimum; TEE = Terminal Eocene Event; MMCO = Middle Miocene Climatic Optimum.

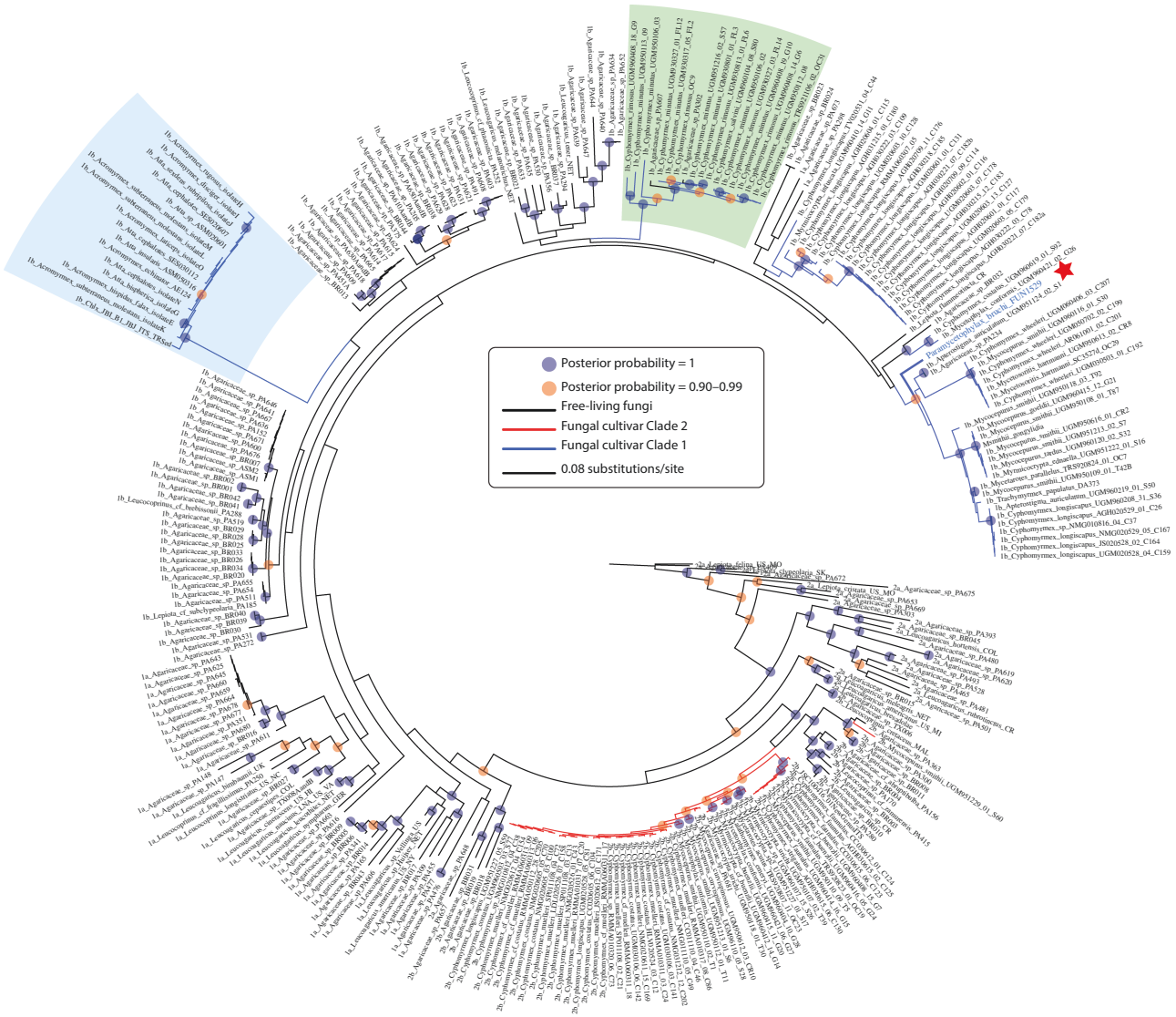

Fig. 9. Phylogeny of fungal cultivars and free-living fungi based on Bayesian analysis of the ITS 'fungal barcoding' region conducted in MrBayes (Ronquist et al. 2012). Ant-cultivated fungi are divided into two clades, Clade 2 (red branches) and Clade 1 (blue branches); free-living fungi are represented by black branches. The cultivar of *Paramycetophylax bruchi* is represented with a blue font and a red star. Nodes with posterior probability of 1 are represented by a blue circle, whereas nodes with posterior probabilities between 0.90 and 0.99 are represented by an orange circle. Nodes without circles indicate posterior probabilities lower than 0.90. Green box indicates the clade of fungi cultivated by the yeast-growing ants in the genus *Cyphomyrmex* and the blue box indicates the clade of fungi cultivated by the leaf-cutting ants and *Apterostigma megacephala*.

Supplementary Data

Supplementary data are available at *Insect Systematics and Diversity* online.

Acknowledgments

We thank the Administración de Parques Nacionales, Dirección de Recursos Naturales Renovables, Gobierno de Mendoza, and Dirección Nacional de Biodiversidad for granting research permits. We thank Katie Murphy (Smithsonian Institution National Museum of Natural History Laboratories of Analytical Biology) for help with quality control of pools and for a MiSeq run; E. Okonski and R. Pol for help with logistics; C. I. Paris and A. Saint Esteven for information about *P. bruchi* in San Juan; and the park rangers and employees of APN and RBÑ, especially Pablo D. Waisman, Patricia Slavutzky, Daniel Figueroa, José Aramayo, Abraham Rojas, and Soledad Rojas, for their help with logistics, transport, and accommodations during fieldwork. We thank E. Zoppas de Albuquerque, two anonymous reviewers, and the editor, G. Camacho, for comments and suggestions that helped to improve our manuscript. Research by P.E.H. was supported by Consejo Nacional de Investigaciones Científicas y Técnicas (CONICET); research by T.R.S. and J.S.-C. was supported by the National Science Foundation (NSF) Grant DEB 1927161; and research by T.R.S., P.E.H., and J.S.-C. was supported by an award from the Smithsonian Institute for Biodiversity Genomics and the NMNH Global Genome Initiative.

Author Contributions

PEH: Conceptualization; Data curation; Investigation; Methodology; Visualization; Writing—original draft; Writing—review & editing. JS-C: Conceptualization; Data curation; Formal analysis; Investigation; Methodology; Visualization; Writing—original draft; Writing—review & editing. TRS: Conceptualization; Formal analysis; Funding acquisition; Investigation; Methodology; Project administration; Resources; Supervision; Writing— review & editing.

References Cited

Alvarez, J. A., and P. E. Villagra. 2009. *Prosopis flexuosa* DC. (Fabaceae, Mimosoideae). Kurtziana 35: 49–63.

Bankevich, A., S. Nurk, D. Antipov, A. A. Gurevich, M. Dvorkin, A. S. Kulikov, V. M. Lesin, S. I. Nikolenko, S. Pham, A. D. Prjibelski, et al. 2012. SPAdes:

a new genome assembly algorithm and its applications to single-cell sequencing. J. Comput. Biol. 19: 455–477.

Baroni Urbani, C. 1980. First description of fossil gardening ants (Amber Collection Stuttgart and Natural History Museum Basel; Hymenoptera: Formicidae. I: Attini). Stuttg. Beitr. Nat. B Geol. Paläontol. 54: 1–13.

Blaimer, B. B., P. S. Ward, T. R. Schultz, B. L. Fisher, and S. G. Brady. 2018. Paleotropical diversification dominates the evolution of the hyperdiverse ant tribe Crematogastrini (Hymenoptera: Formicidae). Insect Syst. Divers. 2: 1–14.

Bolger, A. M., M. Lohse, and B. Usadel. 2014. Trimmomatic: a flexible trimmer for Illumina sequence data. Bioinformatics 30: 2114–2120.

Bolton, B. 2021. An online catalog of the ants of the world. (https://antcat.org). (Accessed 29 September 2021).

Borowiec, M. L. 2019a. Convergent evolution of the army ant syndrome and congruence in big-data phylogenetics. Syst. Biol. 68: 642–656.

Borowiec, M. L. 2019b. Spruceup: fast and flexible identification, visualization, and removal of outliers from large multiple sequence alignments. J Open Source Softw. 4: 1635.

Brandão, C. R. F., and A. J. Mayhé-Nunes. 2001. A new fungus-growing ant genus, *Mycetagroicus* gen. n., with the description of three new species and comments on the monophyly of the Attini (Hymenoptera: Formicidae). Sociobiology 38: 639–665.

Branstetter, M. G., A. Ješovnik, J. Sosa-Calvo, M. W. Lloyd, B. C. Faircloth, S. G. Brady, and T. R. Schultz. 2017a. Dry habitats were crucibles of domestication in the evolution of agriculture in ants. Proc. R Soc. Lond. B Biol. Sci. 284: 20170095.

Branstetter, M. G., J. T. Longino, P. S. Ward, and B. C. Faircloth. 2017b. Enriching the ant tree of life: enhanced UCE bait set for genome-scale phylogenetics of ants and other Hymenoptera. Methods Ecol. Evol. 8: 768–776.

Branstetter, M. G., A. Müller, T. L. Griswold, M. C. Orr, and C. D. Zhu. 2021. Ultraconserved element phylogenomics and biogeography of the agriculturally important mason bee subgenus *Osmia* (*Osmia*). Syst. Entomol. 46: 453–472.

Brown, J. M., S. M. Hedtke, A. R. Lemmon, and E. M. Lemmon. 2010. When trees grow too long: investigating the causes of highly inaccurate bayesian branch-length estimates. Syst. Biol. 59: 145–161.

Brown, A., U. M. Ortiz, M. Acerbi, and J. Corcuera. (eds.). 2005. La situación ambiental Argentina. Fundación Vida Silvestre, Buenos Aires.

Bruniard, E. D. 1982. La diagonal árida Argentina: Un límite climático real. Rev. Geogr. 95: 5–20.

Bucher, E. H. 1974. Observaciones ecológicas sobre los artrópodos del bosque chaqueño de Tucumán. Rev. Fac. Cienc. Exact. Fís. Nat. Córdoba (nueva ser.) Cienc. Biol. 1: 35–122.

Cabrera, A. L., and A. Willink. 1980. Biogeografía de América Latina, OEA. Serie de Biología, Washington, DC.

Carpenter, F. M. 1930. The fossil ants of North America. Bull. Mus. Comp. Zool. 70: 1–66.

Castresana, J. 2000. Selection of conserved blocks from multiple alignments for their use in phylogenetic analysis. Mol. Biol. Evol. 17: 540–552.

Chernomor, O., A. von Haeseler, and B. Q. Minh. 2016. Terrace aware data structure for phylogenomic inference from supermatrices. Syst. Biol. 65: 997–1008.

Cristiano, M. P., D. C. Cardoso, V. E. Sandoval-Gómez, and F. C. Simões-Gomes. 2020. *Amoimyrmex* Cristiano, Cardoso and Sandoval, gen. nov. (Hymenoptera: Formicidae): a new genus of leaf-cutting ants revealed by multilocus molecular phylogenetic and morphological analyses. Aust. Entomol. 59: 643–676.

Cuezzo, F. 1998. Formicidae, pp. 452–462. *In* J. J. Morrone and S. Coscaron (eds.), Biodiversidad de artrópodos argentinos, una perspectiva biotaxonómica. Ediciones Sur, La Plata, Argentina.

Diehl-Fleig, Ed. and E. Diehl. 2007. Nest architecture and colony size of the fungus-growing ant *Mycetophylax simplex* Emery, 1888 (Formicidae, Attini). Insectes Soc. 54: 242–247.

Economo, E. P., P. Klimov, E. M. Sarnat, B. Guénard, M. D. Weiser, B. Lecroq, and L. L. Knowles. 2015. Global phylogenetic structure of the hyperdiverse ant genus *Pheidole* reveals the repeated evolution of macroecological patterns. Proc. Biol. Sci. 282: 20141416.

Economo, E. P., J.-P. Huang, G. Fischer, E. M. Sarnat, N. Narula, M. Janda, B. Guénard, J. T. Longino, and L. L. Knowles. 2019. Evolution of the latitudinal diversity gradient in the hyperdiverse ant genus *Pheidole*. Glob. Ecol. Biogeogr. 28: 456–470.

Faircloth, B. C. 2013. Illumiprocessor: a trimmomatic wrapper for parallel adapter and quality trimming. (http://dx.doi.org/10.6079/J9ILL).

Faircloth, B. C. 2016. PHYLUCE is a software package for the analysis of conserved genomic loci. Bioinformatics 32: 786–788.

Faircloth, B. C., and T. C. Glenn. 2012. Not all sequence tags are created equal: designing and validating sequence identification tags robust to indels. PLoS One 7: e42543.

Faircloth, B. C., M. G. Branstetter, N. D. White, and S. G. Brady. 2015. Target enrichment of ultraconserved elements from arthropods provides a genomic perspective on relationships among Hymenoptera. Mol. Ecol. Resour. 15: 489–501.

Fisher, S., A. Barry, J. Abreu, B. Minie, J. Nolan, T. M. Delorey, G. Young, T. J. Fennell, A. Allen, L. Ambrogio, et al. 2011. A scalable, fully automated process for construction of sequence-ready human exome targeted capture libraries. Genome Biol. 12: R1.

Glenn, T. C., R. A. Nilsen, T. J. Kieran, J. G. Sanders, N. J. Bayona-Vásquez, J. W. Finger, T. W. Pierson, K. E. Bentley, S. L. Hoffberg, S. Louha, et al. 2019. Adapterama I: Universal stubs and primers for 384 unique dual-indexed or 147, 456 combinatorially-indexed Illumina libraries (iTru & iNext). PeerJ 7: e7755.

Guindon, S., J. F. Dufayard, V. Lefort, M. Anisimova, W. Hordijk, and O. Gascuel. 2010. New algorithms and methods to estimate maximum-likelihood phylogenies: assessing the performance of PhyML 3.0. Syst. Biol. 59: 307–321.

Hoang, D. T., O. Chernomor, A. von Haeseler, B. Q. Minh, and L. S. Vinh. 2018. UFBoot2: improving the ultrafast bootstrap approximation. Mol. Biol. Evol. 35: 518–522.

Ješovnik, A., J. Sosa-Calvo, C. T. Lopes, H. L. Vasconcelos, and T. R. Schultz. 2013. Nest architecture, fungus gardens, queen, males and larvae of the fungus-growing ant *Mycetagroicus inflatus* Brandão & Mayhé-Nunes. Insectes Soc. 60: 531–542.

Ješovnik, A., J. Sosa-Calvo, M. W. Lloyd, M. G. Branstetter, F. Fernández, and T. R. Schultz. 2017. Phylogenomic species delimitation and host-symbiont coevolution in the fungus-farming ant genus *Sericomyrmex* Mayr (Hymenoptera: Formicidae): ultraconserved elements (UCEs) resolve a recent radiation. Syst. Entomol. 42: 523–542.

Ješovnik, A., J. Chaul, and T. R. Schultz. 2018. Natural history and nest architecture of the fungus-farming ant genus *Sericomyrmex* (Hymenoptera: Formicidae). Myrmecol. News 26: 65–80.

Kalyaanamoorthy, S., B. Q. Minh, T. K. F. Wong, A. von Haeseler, and L. S. Jermiin. 2017. ModelFinder: fast model selection for accurate phylogenetic estimates. Nat. Methods 14: 587–589.

Karlin, U. O., M. S. Karlin, R. M. Zapata, R. O. Coirini, A. M. Contreras, and M. Carnero. 2017. La Provincia Fitogeográfica del Monte: límites territoriales y su representación. Multequina 26: 63–75.

Katoh, K., and D. M. Standley. 2013. MAFFT multiple sequence alignment software version 7: improvements in performance and usability. Mol. Biol. Evol. 30: 772–780.

Katoh, K., and D. M. Standley. 2014. MAFFT: iterative refinement and additional methods, pp. 131–146. *In* D. Russell (ed.), Multiple sequence alignment methods. Methods in molecular biology (methods and protocols). Humana Press, Totowa, NJ.

Katoh, K., K. Kuma, H. Toh, and T. Miyata. 2005. MAFFT version 5: improvement in accuracy of multiple sequence alignment. Nucleic Acids Res. 33: 511–518.

Katoh, K., J. Rozewicki, and K. D. Yamada. 2019. MAFFT online service: multiple sequence alignment, interactive sequence choice and visualization. Brief. Bioinform. 20: 1160–1166.

Kempf, W. W. 1965. A revision of the Neotropical fungus-growing ants of the genus *Cyphomyrmex* Mayr. Part II: group of *rimosus* (Spinola) (Hym., Formicidae). Stud. Entomol. 8:161–200.

Klingenberg, C., and C. R. F. Brandão. 2009. Revision of the fungus-growing ant genera *Mycetophylax* Emery and *Paramycetophylax* Kusnezov rev. stat., and description of *Kalathomyrmex* n. gen. (Formicidae: Myrmicinae: Attini). Zootaxa 2052: 1–31.

Klingenberg, C., C. R. F. Brandão, and W. Engels. 2007. Primitive nest architecture and small monogynous colonies in basal Attini inhabiting sandy beaches of southern Brazil. Stud. Neotrop. Fauna Environ. 42: 121–126.

Kusnezov, N. 1956. Claves para la identificación de las hormigas de la fauna Argentina. IDIA, Ministerio de Agricultura y Ganadería, Buenos Aires, Argentina.

Lanfear, R., P. B. Frandsen, A. M. Wright, T. Senfeld, and B. Calcott. 2017. PartitionFinder 2: new methods for selecting partitioned models of evolution for molecular and morphological phylogenetic analyses. Mol. Biol. Evol. 34: 772–773.

Leal, I. R., and P. S. Oliveira. 2000. Foraging ecology of attine ants in a Neotropical savanna: seasonal use of fungal substrate in the cerrado vegetation of Brazil: Insectes Soc. 47: 376–382.

Li, H., J. Sosa-Calvo, H. A. Horn, M. T. Pupo, J. Clardy, C. Rabeling, T. R. Schultz, and C. R. Currie. 2018. Convergent evolution of complex structures for ant-bacterial defensive symbiosis in fungus-farming ants. Proc. Natl. Acad. Sci. USA 115: 10720–10725.

Lugo, A. E., E. G. Farnworth, D. Pool, P. Jerez, and G. Kaufman. 1973. The impact of the Leaf-cutter ant A*tta colombica* on the energy flow of a tropical west forest. Ecology. 54: 1292–1301.

Marshall, D. C. 2010. Cryptic failure of partitioned Bayesian phylogenetic analyses: lost in the land of long trees. Syst. Biol. 59: 108–117.

Marshall, D. C., C. Simon, and T. R. Buckley. 2006. Accurate branch length estimation in partitioned Bayesian analyses requires accommodation of among-partition rate variation and attention to branch length priors. Syst. Biol. 55: 993–1003.

Masiulionis, V. E., C. Rabeling, H. H. De Fine Licht, T. Schultz, M. Bacci, Jr., C. M. Bezerra, and F. C. Pagnocca. 2014. A Brazilian population of the asexual fungus-growing ant *Mycocepurus smithii* (Formicidae, Myrmicinae, Attini) cultivates fungal symbionts with gongylidia-like structures. PLoS One 9: e103800.

Mehdiabadi, N. J., and T. R. Schultz. 2010. Natural history and phylogeny of the fungus-farming ants (Hymenoptera: Formicidae: Myrmicinae: Attini). Myrmecol. News 13: 37–55.

Mehdiabadi, N.J., U. G. Mueller, S. G. Brady, A. G. Himler, and T. R. Schultz. 2012. Symbiont fidelity and the origin of species in fungus-growing ants. Nat. Commun. 3: 1–7.

Milesi, F. A., and J. L. D. Casenave. 2004. Unexpected relationships and valuable mistakes: non-myrmecochorous *Prosopis* dispersed by messy leaf-cutting ants in harvesting their seeds. Austral Ecol. 29: 558–567.

Miller, M. A., W. Pfeiffer, and T. Schwartz. 2010. Creating the CIPRES science gateway for inference of large phylogenetic trees, pp. 1–8. *In* Proceedings of the Gateway Computing Environments Workshop (GCE), 14 November 2010, New Orleans.

Minh, B. Q., H. A. Schmidt, O. Chernomor, D. Schrempf, M. D. Woodhams, A. von Haeseler, and R. Lanfear. 2020. IQ-TREE 2: new models and efficient methods for phylogenetic inference in the genomic era. Mol. Biol. Evol. 37: 1530–1534.

Moreau, C. S. 2008. Unraveling the evolutionary history of the hyperdiverse ant genus *Pheidole* (Hymenoptera: Formicidae). Mol. Phylogenet. Evol. 48: 224–239.

Moreira, A. A., L. C. Forti, M. A. C. Boaretto, A. P. P. Andrade, J. F. S. Lopes, and V. M. Ramos. 2004. External and internal structure of *Atta bisphaerica* Forel (Hymenoptera: Formicidae) nests. J. Appl. Entomol. 128: 204–211.

Mueller, U. G., S. A. Rehner, and T. R. Schultz. 1998. The evolution of agriculture in ants. Science 281: 2034–2038.

Naser-Khdour, S., B. Q. Minh, W. Zhang, E. A. Stone, and R. Lanfear. 2019. The prevalence and impact of model violations in phylogenetic analysis. Genome Biol. Evol. 11: 3341–3352.

Nurk, S., A. Bankevich, D. Antipov, A. Gurevich, A. Korobeynikov, A. Lapidus, A. Prjibelsky, A. Pyshkin, A. Sirotkin, and Y. Sirotkin. 2013. Assembling genomes and mini-metagenomes from highly chimeric reads, 158–170. *In* M. Deng, R. Jiang, F. Sun, and X. Zhang, (eds.), Research in computational molecular biology, RECOMB 2013. Springer, Berlin, Heidelberg.

Ojeda, R. A., C. M. Campos, J. M. Gonnet, C. E. Borghi, and V. G. Roig. 1998. The MaB Reserve of Ñacuñán, Argentina: its role in understanding the Monte Desert biome. J. Arid Environ. 39: 299–313.

Prothero, D. R. 1994. The late eocene-oligocene extinctions. Annu. Rev. Earth Planet Sci. 22: 145–165.

Puttick, M. N. 2019. MCMCtreeR: functions to prepare MCMCtree analyses and visualize posterior ages on trees. Bioinformatics 35: 5321–5322.

Rabeling, C., M. Verhaagh, and W. Engels. 2007. Comparative study of nest architecture and colony structure of the fungus-growing ants, *Mycocepurus goeldii* and *M. smithii*. J. Insect Sci. 7: 1–13.

Rambaut, A., A. J. Drummond, D. Xie, G. Baele, and M. A. Suchard. 2018. Posterior summarization in bayesian phylogenetics using tracer 1.7. Syst. Biol. 67: 901–904.

Ronque, M. U. V., R. M. Feitosa, and P. S. Oliveira. 2019. Natural history and ecology of fungus-farming ants: a field study in Atlantic rainforest. Insectes Soc. 66: 375–387.

Ronquist, F., M. Teslenko, P. van der Mark, D. L. Ayres, A. Darling, S. Höhna, B. Larget, L. Liu, M. A. Suchard, and J. P. Huelsenbeck. 2012. MrBayes 3.2: efficient Bayesian phylogenetic inference and model choice across a large model space. Syst. Biol. 61: 539–542.

Rossi, B. E., and P. E. Villagra. 2003. Effects of *Prosopis flexuosa* on soil properties and the spatial pattern of understory species in arid Argentina. J. Veg. Sci. 14: 543–550.

Santschi, F. 1916. Formicides sudaméricains nouveaux ou peu connus. Physis 2: 365–399.

Schultz, T. R., and S. G. Brady. 2008. Major evolutionary transitions in ant agriculture. Proc. Natl. Acad. Sci. USA 105: 5435–5440.

Schultz, T. R., J. Sosa-Calvo, S. G. Brady, C. T. Lopes, U. G. Mueller, M. Bacci, Jr., and H. L. Vasconcelos. 2015. The most relictual fungus-farming ant species cultivates the most recently evolved and highly domesticated fungal symbiont species. Am. Nat. 185: 693–703.

Sela, I., H. Ashkenazy, K. Katoh, and T. Pupko. 2015. GUIDANCE2: accurate detection of unreliable alignment regions accounting for the uncertainty of multiple parameters. Nucleic Acids Res. 43: W7–14.

Snelling, R. R., and J. T. Longino. 1992. Revisionary notes on the fungus-growing ants of the genus *Cyphomyrmex*, *rimosus* group (Hymenoptera: Formicidae: Attini), pp. 479–494. *In* D. Quintero, and A. Aiello (eds.), Insects of Panama and Mesoamerica: selected studies. Oxford University Press, Oxford, United Kingdom.

Solomon, S. E., C. T. Lopes, U. G. Mueller, A. Rodrigues, J. Sosa-Calvo, T. R. Schultz, and H. L. Vasconcelos. 2011. Nesting biology and fungiculture of the fungus-growing ant, *Mycetagroicus cerradensis*: New light on the origin of higher attine agriculture. J. Insect Sci. 11: 1–14.

Solomon, S. E., C. Rabeling, J. Sosa-Calvo, C. T. Lopes, A. Rodrigues, H. L. Vasconcelos, M. Bacci Jr., U. G. Mueller, and T. R. Schultz. 2019. The molecular phylogenetics of *Trachymyrmex* Forel ants and their fungal cultivars provide insights into the origin and coevolutionary history of 'higher-attine' ant agriculture. Syst. Entomol. 44: 939–956.

Sosa-Calvo, J., T. R. Schultz, C. R. Brandão, C. Klingenberg, R. M. Feitosa, C. Rabeling, M. Bacci, Jr., C. T. Lopes, and H. L. Vasconcelos. 2013. *Cyatta abscondita*: taxonomy, evolution, and natural history of a new fungus-farming ant genus from Brazil. PLoS One 8: e80498.

Sosa-Calvo, J., A. Ješovnik, E. Okonski, and T. R. Schultz. 2015. Locating, collecting, and maintaining colonies of fungus-farming ants (Hymenoptera: Myrmicinae: Attini). Sociobiology 62: 300–320.

Sosa-Calvo, J., A. Ješovnik, C. T. Lopes, A. Rodrigues, C. Rabeling, M. Bacci Jr., H. L. Vasconcelos, and T. R. Schultz. 2017a. Biology of the relict fungus-farming ant *Apterostigma megacephala* Lattke, including descriptions of the male, gyne, and larva. Insectes Soc. 64: 329–346.

Sosa-Calvo, J., A. Ješovnik, H. L. Vasconcelos, M. Bacci, Jr., and T. R. Schultz. 2017b. Rediscovery of the enigmatic fungus-farming ant '*Mycetosoritis*' asper Mayr (Hymenoptera: Formicidae): Implications for taxonomy, phylogeny, and the evolution of agriculture in ants. PLoS One 12: e0176498.

Sosa-Calvo, J., T. R. Schultz, A. Ješovnik, R. A. Dahan, and C. Rabeling. 2018. Evolution, systematics, and natural history of a new genus of cryptobiotic fungus-growing ants. Syst. Entomol. 43: 549–567.

Sosa-Calvo, J., F. Fernández, and T. R. Schultz. 2019. Phylogeny and evolution of the cryptic fungus-farming ant genus *Myrmicocrypta* F. Smith (Hymenoptera: Formicidae) inferred from multilocus data. Syst. Entomol. 44: 139–162.

Tagliacollo, V. A., and R. Lanfear. 2018. Estimating improved partitioning schemes for ultraconserved elements. Mol. Biol. Evol. 35: 1798–1811.

Talavera, G., and J. Castresana. 2007. Improvement of phylogenies after removing divergent and ambiguously aligned blocks from protein sequence alignments. Syst. Biol. 56: 564–577.

Thorne, J. L., H. Kishino, and I. S. Painter. 1998. Estimating the rate of evolution of the rate of molecular evolution. Mol. Biol. Evol. 15: 1647–1657.

Vo, T. L., U. G. Mueller, and A. S. Mikheyev. 2009. Free-living fungal symbionts (Lepiotaceae) of fungus-growing ants (Attini: Formicidae). Mycologia 101: 206–210.

Ward, P. S., S. G. Brady, B. L. Fisher, and T. R. Schultz. 2015. The evolution of myrmicine ants: phylogeny and biogeography of a hyperdiverse ant clade (Hymenoptera: Formicidae). Syst. Entomol. 40: 61–81.

Weber, N. A. 1958. Some attine synonyms and types (Hymenoptera, Formicidae). Proc. Entomol. Soc. Wash. 60: 259–264.

Weber, N. A. 1966. Fungus-growing ants. Science 153: 587–604.

Weber, N. A. 1982. Fungus ants, pp. 255–363. *In* H. R. Hermann. Social insects. Academic Press, New York.

Wheeler, W. M. 1907. The fungus-growing ants of North America. Bull. Am. Mus. Nat. His. 23: 669–807.

Yang, Z. 2007. PAML 4: phylogenetic analysis by maximum likelihood. Mol. Biol. Evol. 24: 1586–1591.

Yang, Z., and B. Rannala. 1997. Bayesian phylogenetic inference using DNA sequences: a Markov Chain Monte Carlo Method. Mol. Biol. Evol. 14: 717–724.

Zachos, J., M. Pagani, L. Sloan, E. Thomas, and K. Billups. 2001. Trends, rhythms, and aberrations in global climate 65 Ma to present. Science 292: 686–693.